

# 1.1. Bridges' sections

BY FRANK BRIDGES

## 1.1.1. Sample considerations: 3.18

The homogeneity, uniformity, and thickness of the sample are crucial for collecting high quality EXAFS and XANES data. When samples are not prepared appropriately the EXAFS oscillations can be too small in amplitude and structure in the XANES can easily be distorted - and it may not be obvious from looking at the data that a problem exists. These issues are more important for transmission data because of the log function used to calculate the absorption coefficient i.e.  $\mu(E)t = \ln(I_o/I_1)$  where  $\mu(E)$  is the absorption coefficient at energy  $E$ ,  $t$  is the sample thickness,  $I_o$  is the incident flux and  $I_1$  is the transmitted flux. When the sample thickness varies and the incident flux is not uniform, these variations can couple which is particularly important at monochromator induced glitches (Sec. 1.1.1.4). For high energy edges these errors can easily be avoided by careful preparation, but at lower energies which require thinner samples it becomes increasingly difficult to minimize these effects for energies below roughly 5-6 keV.

### 1.1.1.1. Pinholes and particle size

A simple way to understand how sample non-uniformity changes both the EXAFS and the XANES data, is to consider a sample with a single pinhole; then a small fraction  $f$  of the initial beam is not absorbed and passes through the sample, and the measured transmitted flux  $I_1$  is given by

$$I_1 = I_o[(1 - f)\exp(-\mu t) + f]. \quad (1.1.1.1)$$

When the second term  $f$  begins to be a significant fraction of the first term  $[(1-f)\exp(-\mu t)]$ , then the edge becomes distorted. Consider a XANES scan; as  $\mu$  increases through an edge, (and  $\exp(-$

$\mu t)$  decreases), the resulting decrease in  $I_1$  is too small because of the flux through the pinhole. The larger  $\mu$  becomes, the more the change in  $I_1$  becomes compressed, with a larger compression at the top of the edge but relatively little compression near the bottom. For EXAFS, the oscillation amplitude will also be too small, as the top of the edge (including the EXAFS range) is the most compressed region while the measured edge step, used for normalization, is relatively too large. More formally, defining  $(\mu^*t) = \ln(I_o/I_1)$  as the measured value, then we can expand Eqn. 1.1.1.1 for  $f\exp(\mu t) < 1$  to give the ratio  $R = (\mu^*t)/(\mu t)$  as:

$$R = (\mu^*t)/(\mu t) \approx 1 - f(\exp(\mu t) - 1)/(\mu t). \quad (1.1.1.2)$$

For  $f = 0.01$ , this is a good approximation up to  $\mu t \approx 3$ . As  $\mu t$  increases,  $R$  decreases from 1.0 - at first linearly, but then faster. This compresses the data at high  $\mu t$  as discussed above.

Note that the thicker the sample, the faster the term  $f\exp(\mu t)$  increases with  $\mu$ , and the larger the distortion. Stern & Kim (1981) have explored this effect in some detail but focused more on the measured EXAFS function  $\chi^*$  (determined by small variations in  $\mu^*t$ ), and the measured step height  $\mu_e^*t$ , when background absorption below the edge is small.

The ratio of the measured value to the actual value of  $\chi$ , i.e.  $\chi^*/\chi$ , approaches 1.0 as the actual edge step height  $\mu_e t$  decreases to 0. Stern and Kim plot the ratios  $\chi^*/\chi$  and  $\mu_e^*t/\mu_e t$  for a range of values of  $f$  and  $\mu_e t$ , but don't consider the effects of a significant background from other atoms in the sample. Since many materials currently being investigated often have a significant absorption background, we expand these calculations below.

First set  $\mu = \mu_o + \mu_e$  in Equ. 1.1.1.1, where  $\mu_o$  is the background absorption coefficient and  $\mu_e t$  is the edge step. Then the measured step height  $\mu_e^*t$  is obtained by subtracting  $\mu_o^*t$  from  $\mu^*t$ :

$$(\mu_e^*t) = -\ln[(1 - f)\exp(-(\mu_o + \mu_e)t) + f] + \ln[(1 - f)\exp(-(\mu_o t)) + f] \quad (1.1.1.3)$$

and the ratio of the measured step height to the actual step height is  $\mu_e^*t/\mu_e t = \mu_e^*/\mu_e$ . In Fig. 1.1.1.1 we plot  $\mu_e^*/\mu_e$  as a function of the actual step height ( $\mu_e t$ ), for four values of  $f$  (0.005, 0.01, 0.02, 0.04) and two values of  $\mu_o t$  (1.0 and 2.0). This ratio decreases with increasing  $\mu_o t$ , and with increasing  $f$ ; it is also very dependent on the value of  $\mu_e t$ , even for  $\mu_o t = 1.0$ . Thus pinholes have an even larger effect when the sample is relatively thick, and the background absorption is comparable to or larger than  $\mu_e t$ . It is therefore important to determine the absorption from the other atoms in the sample.

*proportionally*

*fractionally*

*z Δμ? Δμt?*

*some starting data: plot μ\_e^\*/μ\_e vs μ\_e t for f = 0.005, 0.01, 0.02, 0.04 and μ\_o t = 1.0, 2.0*

*approximate data set*

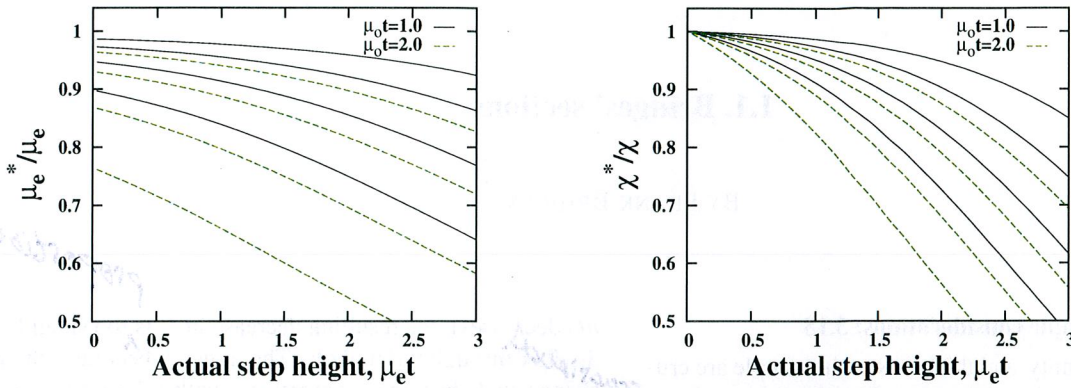


Fig. 1.1.1.1. The ratios  $\mu_e^*/\mu_e$  (Left) and  $\chi^*/\chi$  (Right) as a function of the actual step height ( $\mu_e t$ ) for different values of the pinhole fraction  $f$  from 0.005 to 0.04 and for  $\mu_o t = 1.0$  (solid lines) and 2.0 (dashed lines).  $f$  increases downward.

To obtain the experimental EXAFS oscillation function  $\chi$ , Stern & Kim (1981) considered a small change,  $\Delta\mu_e^* t$ , of  $\mu_e^* t$  above the edge, and defined  $\chi$  as  $\Delta\mu_e/\mu_e$  and  $\chi^*$  as  $\Delta\mu_e^*/\mu_e^*$ . Then from Eqn. 1.1.1.3

$$(\Delta\mu_e^* t) = \frac{1}{(1-f)\exp(-(\mu_o + \mu_e)t) + f} ((1-f)\exp(-(\mu_o + \mu_e)t)) (\Delta\mu_e t)$$

$$\frac{\chi^*}{\chi} = (\Delta\mu_e^* t) \mu_e t / ((\Delta\mu_e t) \mu_e^* t) \tag{1.1.1.4}$$

In Fig. 1.1.1.1:Right,  $\chi^*/\chi$  is plotted as a function of actual step height for the same values of  $f$  and  $\mu_o t$ . Even when the step height is only 1.0, there is a significant suppression of  $\chi^*$  when the pinhole leakage is a few percent; and if the background absorption  $\mu_o t$  is as large as 2.0, it can be a 20 % effect. In comparing with Stern & Kim (1981), the results in Fig. 1.1.1.1 show a larger suppression of  $\chi^*/\chi$  and  $\mu_e^*/\mu_e$  than in Fig. 1 of their paper. Although the notation is slightly different, if Eqs. 1.1.1.3 and 1.1.1.4 are plotted with  $\mu_o t \sim 0$ , then the results in Fig. 1.1.1.1 are the same as Fig. 1 in Stern & Kim (1981).

For many samples studied currently, the unit cell usually contains several elements and then one must also consider the background absorption of these other atoms. This background can be large and can't be ignored; it may require that the step height be much less than 1.0 when pinholes are present.

Since partial pinhole effects (i.e. thin sections of samples, cracks, etc.) cannot be completely eliminated for powder samples, it is best not to use thick samples. Goulon *et al.* (1982) have also noted the important effect of leakage through the sample in their analysis of errors in the collection of EXAFS data.

Typically we keep the edge step height ( $\Delta\mu t$ ) in the range 0.3-0.7, to minimize such pinhole effects, but for moderately low concentrations (3-10 %) for the element of interest, it is useful to check two different sample thicknesses to verify that the step height is proportional to sample thickness. If the samples are fairly uniform, an easy way to do so is to collect XANES data with the sample rotated at different angle relative to the x-ray beam – e.g perpendicular to beam and at 45°. For these angles the step height should be 1.4 times larger at 45°. If it is smaller then there are pinhole problems.

A more general equation for  $I_1$  when both the incident flux and sample thickness are not uniform is given by:

$$I_1(E) = \int I_o(x, y) \exp(-\mu(E)t(x, y)) dx dy \tag{1.1.1.5}$$

where  $I_o(x, y)$  and  $t(x, y)$  are the incident flux and sample thickness at point  $(x, y)$  within the x-ray beam area. One important example of using this equation is usually referred to as the particle size effect (Lu & Stern, 1983). Consider a single layer of close packed particles of diameter  $D$ . The center of each particle will be highly absorbing if  $D$  is large, while the edges transmit significantly more flux, much like a partial pinhole. Lu & Stern (1983) calculated the transmission through such a particle and treated other leakage flux as discussed above. They showed that if the particle size is too large there is a serious reduction in the EXAFS amplitude (and also a distortion of the XANES although not discussed). How thick is too thick depends on the absorption length at the edge of interest for a given sample. The diameter of the particles should be much less than this absorption length. Using nearly identical layers of particles (formed by rubbing fine particles onto scotch tape) they showed that the error is small if the absorption edge step per layer is 0.1 or less. This is a strong constraint on the particle size, particularly for energies below  $\sim 5-6$  keV, as the decrease of  $\chi^*/\chi$  below 1.0 grows as the x-ray energy decreases for a given value of  $D$ . Note also that using small particles reduces pinhole effects

*this isn't about us*

*Note: add particle size est. to calc!*

→ that only make sense for tape, which wasn't been mentioned  
 1.1. BRIDGES' SECTIONS waaa! too small!

between particles and using many layers further reduces pinhole effects. Thus it is best to use very fine powders in making samples - usually < 5 micron and for low energies, down to 1 micron. Finally since the EXAFS oscillations are small and the compression does not change much over an oscillation, the measured EXAFS are to a good approximation given by  $\chi^* = \alpha\chi$  where  $\alpha$  is a constant. This is effectively a reduction of the parameter  $S_0^2$  by  $\alpha$ , and likely contributes in part to variations of the reported values of  $S_0^2$  for a

given element in the literature.

1.1.1.2. Tapered samples and non-uniform x-ray flux

A second example using Eqn. 1.1.1.5 is for tapered samples when the x-ray flux also varies across the beam. Assume there is a linear taper of thickness along the x-direction and that the x-ray flux also varies in this direction; for simplicity let it be a linear variation and assume no variation along y. Then:

→ Not quite sure of audience... do we need to prove things? or just cite them?

$$I_0(x) = I_0(1 + \beta x); \quad t(x) = t_0(1 + \gamma x)$$

$$I_1(E) = \int I_0(1 + \beta x) \exp(-\mu(E)(t_0(1 + \gamma x))) dx \quad (1.1.1.6)$$

something subtracted wrong

where  $I_0$  and  $t_0$  are average values of the incident flux and sample thickness,  $\beta$  and  $\gamma$  are small constants describing the linear variations, and the range of integration is [-0.5:0.5] for 1 mm slit height; if the slits are smaller the effects are smaller. Carrying out the integration under the assumption that  $\mu t_0 \gamma x$  is small then  $I_1(E)$  and  $(\mu t)^*$  are approximately given by:

$$I_1(E) = I_0 \exp(-\mu t_0) (1 - \mu t_0 \beta \gamma / 12)$$

$$(\mu t)^* = \mu t_0 (1 + \beta \gamma / 12) \quad (1.1.1.7)$$

do you need to cite something?

Thus  $(\mu t)^*$  can be slightly smaller or larger than the value  $(\mu t_0)$  (calculated using the average thickness), depending on the signs of  $\beta$  and  $\gamma$ . If the highest flux passes through the thickest part of the sample then the absorption is larger, whereas if the highest flux passes through the thinnest section of the sample, it will be lower. The effects for  $\chi^*$  are similar but the equations somewhat more complex particularly if the background value of  $\mu$  below the edge, is significant. The important point to note is that if there are large spatial variations in the flux and the sample is tapered the extracted  $\chi^*$  can differ from the real value. Since x-ray beams at synchrotrons can have significant variations (for side stations there is a large horizontal variation in flux, and for focused beams there is a large variation across the beam in both the x- and y-directions unless small slits are used and positioned appropriately), it is important to minimize variations in thickness. In general the beam position can also vary slightly with time and/or with energy. If for example the highest intensity of the beam shifts towards (away from) a pinhole from one data point to the next, the  $I_1$  intensity will increase (decrease) and that will appear as noise in the scan. Similar issues can occur if  $\mu$  is also a function of  $x$  and  $y$  - e.g. in soil or powdered rock samples; then the distribution of distinct compounds in the samples can vary dramatically across the sample. If the x-ray beam is also not uniform across the beam, then the step height for a given element might not be a good measure of the relative concentration of the corresponding compound.

Focus on tapered should be non-uniform

More complicated variations of sample thickness need to be addressed on a case by case basis. For example Ottaviano *et al.* (1994) have considered the more complex case of a distribution of metallic particles of different diameters embedded in a matrix.

They estimated the particle size distribution from microscope pictures and then modeled the transmission of this composite to extract a measure of  $\mu$ . For further details see Ottaviano *et al.* (1994).

1.1.1.3. samples for fluorescence measurements

The sample constraints for fluorescence measurements are much less restrictive because the log function is not involved. Uniform sample are always best but other considerations might dictate the form of the sample. If the concentration of the element of interest is low then thick samples can be used as the rest of the sample determines the penetration depth. If pinholes are present that fraction ( $f$ ) of the beam does not produce a fluorescence signal. Then  $I_0$  is not exactly the incident flux (i.e.  $I_0(1-f)$ ) that produces fluorescence. However if the incident flux were uniform across the sample the net fluorescence would only be reduced by  $1-f$  and the XANES and EXAFS would not be changed. If the beam is not uniform and the spatial intensity distribution across the sample varies with time, that can lead to fluctuations that contribute to noise or to longer term drifts which will act like a change in gain with time. Usually this is not very important for unfocused beams, but could be important if a focused beam is used, the slits are not small enough to use just the uniform part of the beam, and the focused beam moves slightly during a scan.

bad

If the concentration of the element of interest is relatively concentrated then self absorption effects must be addressed and corrected (See Sec. 1.1.3). For concentrated samples it is often useful to use a thin sample (compared to an absorption length). However the issues discussed above, when the sample is non-uniform, the beam intensity is non-uniform, and/or some beam motion is present, still apply.

→ do u mean  $\mu t_0$ ? sab correct req. more exact

1.1.1.4. sample inhomogeneity and glitches knowledge otherwise

Variations in sample thickness also play a role in the magnitude of glitches induced by additional Bragg reflections within the monochromator, usually called monochromator glitches (Bridges & Wang, 1991; Bridges *et al.*, 1992; Li *et al.*, 1994). Here we assume that harmonics have been sufficiently removed, and only consider unfocused beams - the behavior of focused beams

beams out of place

3 not explained

depends on the focusing conditions,

*but the principles are the same*

At particular energies (angles) for a given monochromator crystal, three or more Bragg reflections can be simultaneously possible over a small energy range - usually a few eV. Then when an EXAFS scan passes through such an energy, some of the desired x-rays go into another *reflection*, reducing the incident flux in  $I_0$  over a small energy interval. In addition because of the slight divergence of the x-ray beam from a synchrotron as it moves towards the monochromator, the energy varies slightly in the vertical direction - for Si 220 crystals at 20 m from the electron beam, the variation is about 1.4 eV/mm *at* 10 keV (Bridges *et al.*, 1992) and about 2.4 eV/mm for 111 crystals - see Fig. 2 in Li *et al.* (1994). Consequently if the beam profile is scanned vertically over a range of 4 mm, there will be a dip in the profile at the glitch energy (roughly 1-2 mm wide) that moves across the beam profile. An example is shown in Fig. 1.1.1.2; see experimental measurements on two beamlines at SSRL in Figs. 1 of Bridges *et al.* (1992) and Li *et al.* (1994).

*comparing  
to energy*

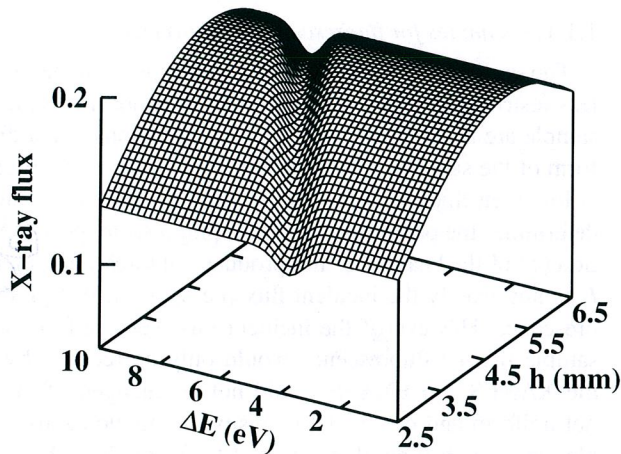


Fig. 1.1.1.2. Simulation of a monochromator glitch crossing a beam profile;  $h$  is the vertical direction and the beam extends from 2.5 to 6.5 mm; this simulation is based on results in Bridges *et al.* (1992) and Li *et al.* (1994). The glitch is a narrow dip on the profile for a vertical scan (using tiny slits, 0.05mm) at a fixed x-ray energy. At  $h = 5$  mm, the slope of the beam within a vertical slit of say 1 mm, will change from zero, to negative, to zero (middle of glitch), to positive, and back to zero, as the energy is increased through the glitch.

To see how this produces the glitch in an EXAFS scan consider Eqn. 1.1.1.6 but with  $x$  now the vertical direction,  $h$ . As this dip moves across the slits (that define the beam), the parameter  $\beta$  changes with increasing energy, from nearly zero to negative to positive and back to nearly zero (or vice versa depending on the beamline configuration). The correction term in Eqn. 1.1.1.7,  $\beta\gamma/12$ , then fluctuates producing the glitch. If the sample is very uniform (i.e.  $\gamma$  which describes any taper is tiny) this effect becomes small; in addition the glitch size can also be significantly reduced by using narrow slits (Bridges *et al.*, 1992). More complex situations can be modeled in a similar way. For focused beams the position and shape of the glitch on the profile, need to be determined.

## 1.1. BRIDGES' SECTIONS

### 1.1.2. Geometry: 3.59

The geometry of the experimental set-up for transmission experiments is straight forward as shown in Fig. 1.1.2.1. Usually it consists of the incident flux detector,  $I_0$ , sample chamber/cryostat, transmitted flux detector,  $I_1$ , reference sample, and  $I_2$ , aligned along the x-ray beam. It's important to center each detector,  $I_i$  on the x-ray beam, and separate the detectors sufficiently that fluorescence flux from the sample chamber/cryostat or the reference sample does not contribute to the signal in either  $I_0$  or  $I_1$ . To quan-

tify this statement let  $A$  be the active area of the windows on each detector; then the fraction of fluorescence flux is  $A/(4\pi r^2)$  where  $r$  is the distance from the sample (or ref. sample) to the detector. It is useful to keep this fraction less than  $10^{-3}$ ; for example if  $A = 3 \text{ cm}^2$  and the detector is 15 cm away from the sample then this fraction is  $1.05 \times 10^{-3}$ . If the detector(s) needs to be closer, the active area  $A$  can be reduced substantially using a smaller slit on the end of the detector; although this slit must be aligned carefully it is usually straightforward because the active beam area is usually less than  $0.1 \text{ cm}^2$ .

*need to say why. In this context, it isn't clear.*

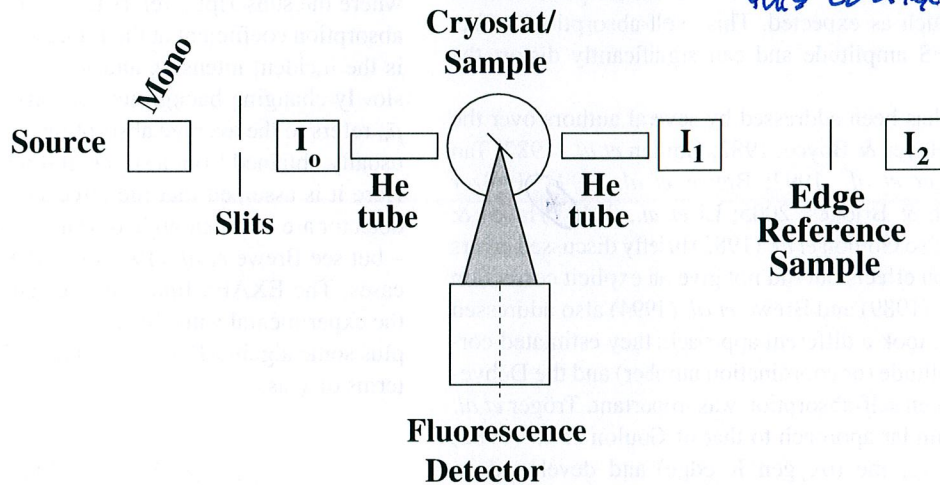


Fig. 1.1.2.1. A typical set-up for both transmission and fluorescence data collection; top view. For transmission there is no fluorescence detector and the sample (in the cryostat or sample holder) is usually perpendicular to the x-ray beam. The spacing between the sample and either  $I_0$  or  $I_1$  must be sufficient that little fluorescent or scattered x-ray flux from the sample can reach these detectors. Similarly the reference sample must be far enough away so no significant flux from the reference sample reaches  $I_1$ . For low energies, including tubes filled with low absorbing helium gas minimizes air absorption. For fluorescence measurements the sample is at  $45^\circ$  to the x-ray beam as shown and the fluorescence is collected in a detector at  $90^\circ$  to the beam. The solid angle collected by this detector is shaded.

*(below 6 keV or so)*

For lower energies, air between the sample and detectors starts to significantly attenuate the x-ray beam. Then it is useful to add a helium-filled tube between the detectors and the sample. For example at 5 keV, 50% of the flux is absorbed in 15 cm of air, while in helium gas less than 1% is absorbed.

For fluorescence measurements the transmission set-up is usually retained and a fluorescence detector added at  $90^\circ$  to the beam, with the sample rotated by  $45^\circ$  as shown in Fig. 1.1.2.1. For fluorescence measurements it is important to minimize elastically scattered radiation - from the sample as well as from the air path on each side of the sample. The latter can be mostly eliminated using helium-filled tubes between the sample and the  $I_0$  and  $I_1$  detectors, but additional shielding might be needed.

Reducing the elastic scattering from the sample is more difficult. Fortunately synchrotrons are linearly polarized in the horizontal direction, and elastic scattering along a line through the sample that is parallel to the polarization axis goes to zero. Fluorescence detectors have a significant subtended solid angle and elastic scattering towards the outer edge of the detector may be significant. Since for many synchrotrons there is often too much flux for current fluorescence detectors, the flux reaching the detector needs to

be limited. This can be achieved by either slitting down the incident beam or by reducing the solid angle subtended by the detector by moving it away from the sample (if  $A_D$  is the area of the detector and  $R$  the distance from the sample to the detector, the solid angle  $\Omega = A_D/(4\pi r^2)$ ). It is desirable to reduce the fluorescence flux by keeping the slits reasonably large (consistent with sample size and required energy resolution, etc.) and moving the detector away from the sample, as this reduces the elastic scattering and usually results in a larger count rate in the fluorescence channel for a fixed incoming total count rate.

*just noting I never appreciated that before*

*\* probably need to reference section on deadtime, wherever that is*

## 1.1.3. Self absorption corrections: 3.65

When all the atoms of interest in a dilute or very thin sample have the same incident flux of x-rays, the number of fluorescence photons is proportional to the photoelectric part of the x-ray absorption coefficient,  $\mu$ . However many samples are not in that limit - the concentration of the atoms of interest may not be low and the sample may be thick. In that case the penetration of the x-rays into the sample depends on the total absorption coefficient - and if  $\mu$  varies rapidly with energy,  $E$ , as is the case for XANES and EXAFS, the mean absorption depth also changes. Then if at some energy  $\mu$  decreases slightly, the x-rays penetrate farther into the sample and excite more atoms; thus the number of fluorescence photons does not decrease as much as expected. This "self-absorption" effect reduces the EXAFS amplitude and can significantly distort the XANES.

Self-absorption has been addressed by several authors over the last few decades. (Hayes & Boyce, 1982; Goulon *et al.*, 1982; Tan *et al.*, 1989; Tröger *et al.*, 1992; Brewe *et al.*, 1994; Pfalzer *et al.*, 1999; Booth & Bridges, 2005; Li *et al.*, 2014) Hayes & Boyce (1982) and also Goulon *et al.* (1982) briefly discussed errors from self-absorption effects but did not give an explicit correction function. Tan *et al.* (1989) and Brewe *et al.* (1994) also addressed self-absorption, but took a different approach; they estimated corrections to the amplitude (or coordination number) and the Debye-Waller factor  $\sigma^2$  when self-absorption was important. Tröger *et al.* (1992) applied a similar approach to that of Goulon *et al.* (1982) for the soft x-ray regime (oxygen K edge) and developed an average correction function to extract the actual EXAFS function  $\chi(k)$  from the experimental function; however the correction was for thick samples and did not include changes in  $\mu$  from the EXAFS oscillations. Booth & Bridges (2005) extended this calculation to include variable sample thicknesses and also included the effects of the EXAFS oscillations; the latter are important when the EXAFS oscillations are large such as in ordered materials at low temperatures, e.g. Cu foil. Other approaches have been developed for specialized cases - Li *et al.* (2014) have considered self-absorption effects in multilayer systems for which refraction and multiple reflections are included, Brewe *et al.* (1994) considered a glancing-emergent-angle geometry, and Pfalzer *et al.* (1999) considered the case of a large solid angle detector.

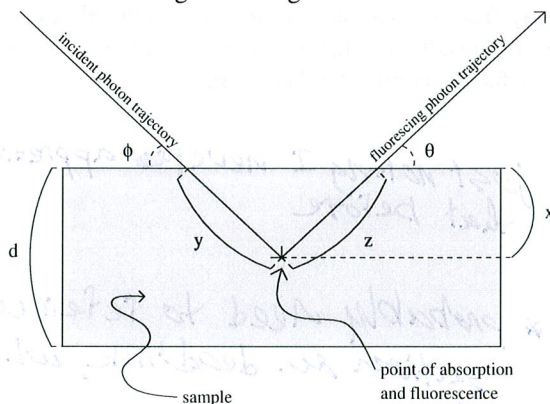


Fig. 1.1.3.1. The geometry for calculating the fluorescence output into a small solid angle in EXAFS and XANES experiments. Often both  $\phi$  and  $\theta$  are  $45^\circ$ . The point for absorption is a distance  $x$  below the surface;  $y$  and  $z$  are distances along the incoming and outgoing photon paths.

Below the self-absorption correction function is developed following the approach of Booth & Bridges (2005); the geometry and some parameters are given in Fig. 1.1.3.1. Defining  $y = x/\sin\phi$  and  $z = x/\sin\theta$ , and integrating over  $x$ , the measured fluorescence intensity  $I_f$  (see Sec. 1.1.2) is given by:

$$I_f(E) = I_o \frac{\epsilon_a \mu_a}{\sin\phi} \int_0^d e^{-(\frac{\mu_T}{\sin\phi} + \frac{\mu_f}{\sin\theta})x} dx$$

$$I_f(E) = I_o \frac{\epsilon_a \mu_a}{\mu_T + g\mu_f} \left[ 1 - e^{-(\frac{\mu_T}{\sin\phi} + \frac{\mu_f}{\sin\theta})d} \right] \quad (1.1.3.8)$$

where the subscript  $a$  refers to the edge of interest,  $\mu_f$  is the total absorption coefficient at the fluorescence energy,  $g = \sin\phi/\sin\theta$ ,  $I_o$  is the incident intensity, and  $\mu_T = \mu_b + \bar{\mu}_a(1 - \chi)$ , with  $\mu_b$  the slowly changing background absorption from other edges/atoms.  $\bar{\mu}_a$  refers to the average absorption above the the edge of interest - usually obtained from a spline fit through the EXAFS oscillations. Here it is assumed that the effects of the finite solid angle of the detector are small enough to be neglected (Booth & Bridges, 2005) - but see Brewe *et al.* (1994) and Pfalzer *et al.* (1999) for special cases. The EXAFS function is given by  $\chi = (\mu_a - \bar{\mu}_a)/\bar{\mu}_a$  and the experimental value by  $\chi_{exp} = (I_f - \bar{I}_f)/\bar{I}_f$ . Using Equ. 1.1.3.8 plus some algebra (Booth & Bridges, 2005),  $\chi_{exp}$  can be written in terms of  $\chi$  as:

$$\chi_{exp} = \left[ \frac{1 - e^{-(\alpha + \chi\bar{\mu}_a)\frac{d}{\sin\phi}}}{1 - e^{-\frac{\alpha d}{\sin\phi}}} \right] \left[ \frac{\alpha(\chi + 1)}{\alpha + \chi\bar{\mu}_a} \right] - 1 \quad (1.1.3.9)$$

where  $\alpha = \bar{\mu}_T + g\mu_f$ . At this point the calculation is exact within the assumption of a uniform thickness (plus a uniform distribution of the atom of interest) and a small detector solid angle. The difficulty with it is that  $\chi_{exp}$  is given as a function of  $\chi$  and cannot be directly inverted to give  $\chi$  as a function of  $\chi_{exp}$ . However, under the assumption that

$$\frac{\chi\bar{\mu}_a d}{\sin\phi} \ll 1 \quad (1.1.3.10)$$

the exponential term in  $\chi$  ( $\exp(-\chi\bar{\mu}_a d/\sin\phi)$ ) can be approximated as  $1 - (\chi\bar{\mu}_a d/\sin\phi)$ , and then Equ. 1.1.3.9 becomes a quadratic equation in  $\chi$ , with a solution:

Ⓢ I think Grant Brunken did some work on this too, esp. re: detector solid angle and the error that introduces into  $\phi \neq \theta$ . Better cover that. Maybe I'm just thinking of Brewe or Pfaltzer, but I think Grant covered particle size effects, too.

## 1.1. BRIDGES' SECTIONS

$$\chi = \frac{-[\gamma(\alpha - \bar{\mu}_a(\chi_{exp} + 1) + \beta) + \sqrt{[\gamma(\alpha - \bar{\mu}_a(\chi_{exp} + 1) + \beta)]^2 + 4\alpha\beta\gamma\chi_{exp}}]}{2\beta}, \quad (1.1.3.11)$$

where

$$\begin{aligned} \gamma &= 1 - e^{-\frac{\alpha d}{\sin\phi}} \\ \beta &= \frac{\bar{\mu}_a \alpha d}{\sin\phi} e^{-\frac{\alpha d}{\sin\phi}}. \end{aligned}$$

The correction factor  $\chi/\chi_{exp}$  now oscillates in  $k$ -space as a result of the EXAFS oscillations. (Booth & Bridges, 2005) This correction has been incorporated into several EXAFS packages such as RSXAP (Booth, 2010) and IFEFFIT. (?) *List stand-alone version?*

### 1.1.3.1. Self-absorption corrections to XANES

The distortion of the XANES from self-absorption is described by the same starting equation as used for EXAFS (Equ. 1.1.3.8) *after* again any background fluorescence has been subtracted. Also, all treatments which we are aware of only consider the infinitely thick limit, for which the exponential term goes to zero. Next, following Haskel (1999), an energy  $E_N$  needs to be chosen above the edge for normalization - it is assumed that this energy is well above the edge and that variations in  $\mu_a$  are small (if not, a point should be chosen on  $\bar{\mu}_a$  e.g. at a "zero-crossing" in the EXAFS oscillations). Then the measured edge is  $I_f(E)/I_o(E)$  and the measured intensity at the normalization energy is  $I_f(E_N)/I_o(E_N)$ . The real edge is  $\mu_a(E)$  and the normalized edge given by  $\mu_a(E)/\mu_a(E_N)$ . Defining the normalized measured edge  $R$  as  $(I_f(E)/I_o(E))/(I_f(E_N)/I_o(E_N))$ , then  $R$  is given by *why R? yuck.*

$$R = \left[ \frac{\mu_a(E)}{\mu_a(E_N)} \right] \left[ \frac{\epsilon_a(E)}{\epsilon_a(E_N)} \right] \left[ \frac{Bg + \delta' + 1}{Bg + \delta + \frac{\mu_a(E)}{\mu_a(E_N)}} \right] \quad (1.1.3.12)$$

where  $B = \mu_f/\mu_a(E_N)$ ,  $\delta = \mu_b(E)/\mu_a(E_N)$ , and  $\delta' = \mu_b(E_N)/\mu_a(E_N)$ . Solving for the actual normalized edge,  $\mu_a(E)/\mu_a(E_N)$ , and simplifying, one obtains (Haskel, 1999)

$$\left[ \frac{\mu_a(E)}{\mu_a(E_N)} \right] = R \left[ \frac{1}{1 + \frac{1-R}{Bg+\delta}} \right]; \quad (1.1.3.13)$$

here it is assumed that for a small energy range about the edge,  $\epsilon_a(E)/\epsilon_a(E_N) \sim 1$ , and  $\delta \sim \delta'$ . Note that Equ. 1.1.3.13 is normalized above the edge -  $R \sim 1$ . Then to have an undistorted edge,  $R$  must be decreased for energies near the bottom of the edge; this correction factor is  $1/[1+1/(Bg+\delta)]$ . In contrast, at a white line in an  $L_{III}$  edge, the correction factor must be greater than one because  $R > 1$ . As long as the correction factor in Equ. 1.1.3.13 is less than 3-4 this is a very good approximation - but if it exceeds 10 as can be the case for Co  $L_{III}$  edge in a cobaltite, the result is questionable.

Booth, C. H., (2010). *R-Space X-ray Absorption Package, 2010*. [Http://lise.lbl.gov/RSXAP/](http://lise.lbl.gov/RSXAP/).

Booth, C. H. & Bridges, F. (2005). *Improved self absorption correction for fluorescence measurements of extended x-ray absorption fine structure*. *Physica Scripta*, **T115**, 202-204. Doi:10.1238/Physica.Topical.115a00202.

Brewe, D. L., Pease, D. M., & Budnick, J. I. (1994). *Corrections of residual fluorescence distortions for a glancing-emergence-angle x-ray-absorption technique*. *Phys. Rev. B*, **50**, 9025-30.

Bridges, F., Li, G. G. & Wang, X. (1992). *Monochromator-induced glitches exafs data i. test of the model for linearly tapered samples*. *Nucl. Inst & Meth. in Phys.* **A320**, 548-555.

Bridges, F. & Wang, X. (1991). *Minimizing 'glitches' in xafs data: A model for glitch formation*. *Nucl. Inst. & Meth. in Phys.* **A307**, 316.

Goulon, J., Goulon-Ginet, C., Cortes, R. & Dubois, J. M. (1982). *On experimental attenuation factors of the amplitude of the XAFS oscillations in absorption, reflectivity and luminescence measurements*. *J. Physique*, **43**, 539-548.

Haskel, D., (1999). *Fluo: correcting xanes for self-absorption in fluorescence data*. [Http://www.aps.anl.gov/haskel/FLUO/fluo.ps](http://www.aps.anl.gov/haskel/FLUO/fluo.ps).

Hayes, T. M. & Boyce, J. B. (1982). *Solid State Physics*, vol. 37, p. 173. New York: Academic.

Li, G. G., Bridges, F. & Wang, X. (1994). *Monochromator induced glitches in exafs data: Ii. test of the model for a pinhole sample*. *Nucl. Instr. and Meth.* **A340**, 420.

Li, W.-B., Yang, X.-Y., Zhu, J.-T., Tu, Y.-C., Mu, B.-Z., Yu, H.-S., Wei, X.-J., Huang, Y.-Y. & Wang, Z.-S. (2014). *Correction method for the self-absorption effects in fluorescence extended x-ray absorption fine structure on multilayer samples*. *Synch. Rad.* **21**, 561-7.

Lu, K.-Q. & Stern, E. A. (1983). *Size effect of powdered sample on exafs amplitude*. *Nucl. Instrum. Meth.* **212**, 475-78.

Ottaviano, L., Filipponi, A. & Cicco, A. D. (1994). *Supercooling of liquid-metal droplets for x-ray-absorption-spectroscopy investigations*. *Phys. Rev. B*, **49**, 11750-58.

Pfalzer, P., Urbach, J.-P., Klemm, M., Horn, S., denBoer, M. L., Frenkel, A. L. & Kirkland, J. P. (1999). *Elimination of self-absorption in fluorescence hard-x-ray absorption spectra*. *Phys. Rev. B*, **60**, 9335-39.

Stern, E. A. & Kim, K. (1981). *Thickness effect on the extended-x-ray-absorption-fine-structure amplitude*. *Phys. Rev. B*, **23**, 3781-87.

Tan, Z., Budnick, J. I. & Heald, S. M. (1989). *Structural parameter determination in fluorescence exafs of concentrated samples*. *Rev. Sci. Instrum.* **60**, 1021-25.

Tröger, L., Arvanitis, D., Baberschke, K., Michaelis, H., Grimm, U. & Zschech, E. (1992). *Full correction of the self-absorption in soft-fluorescence extended x-ray-absorption fine structure*. *Phys. Rev. B*, **46**, 3283-9.

